www.czasopisma.pan.pl PAN POLSKA AKADEMIA NAUK www.journals.pan.pl

Arch. Min. Sci. **66** (2021), 1, 69-84

Electronic version (in color) of this paper is available: http://mining.archives.pl

DOI 10.24425/ams.2021.136693

GÜLNAZ DALOĞLU[1*], MUSTAFA ÖNDER[1], TERESA PARRA[2]

MODELING OF METHANE AND AIR VELOCITY BEHAVIOR IN AN AUXILIARY VENTILATED COAL HEADING

It is commonly known that the cause of serious accidents in underground coal mining is methane. Thus, computational fluid dynamics (CFD) becomes a useful tool to simulate methane dispersion and to evaluate the performance of the ventilation system in order to prevent mine accidents related to methane. In this study, numerical and experimental studies of the methane concentration and air velocity behaviour were carried out. The experiment was conducted in an auxiliary ventilated coal heading in Turkish Hard Coal Enterprises (TTK), which is the most predominant coal producer in Turkey. The simulations were modeled using Fluent-Ansys v.12. Significant correlations were found when experimental values and modeling results were compared with statistical analysis. The CFD modeling of the methane and air velocity in the headings especially uses in auxiliary ventilation systems of places where it is hard to measure or when the measurements made are inadequate.

Keywords: coal mine, methane, computational fluid dynamics (CFD), correlation analysis, ANOVA

1. Introduction

Methane is a gas that is found frequently in underground coal mines and can be linked to many serious accidents. The most devastating mining accidents that occurred in the world are as follows. 1906 one in France caused more than 1000 deaths. Another accident happened in Saint Nicholas, eight coal beds (Spain) resulted in the death of 14 miners. In Russia 103 and 29 miners were killed in 2007 and 2008, respectively. In 2006 13 miners were killed in Ukraine. In China 60, 111, and 74 miners were killed in 2005, 2008 and 2009, respectively. In 2009 in Poland an

[1] ESKIŞEHIR OSMANGAZI ÜNIVERSITESI MÜH. MIM. FAK. MADEN MÜHENDISLIĞI BÖLÜMÜ, 26480 ESKIŞEHIR
[2] UNIVERSITY OF VALLADOLID, DEPARTMENT OF ENERGY AND FLUID MECHANICS, VALLADOLID, SPAIN

* Corresponding author: gdaloglu@ogu.edu.tr

accident caused 8 people to die. Again, in the USA 106 miners were killed in 17 explosions since 1980 [1]. 18 major explosions occurred between 1959 and 1981 in the U.S., twelve of them consisted of methane-air mixtures and this value is 30% of the total accident rate [2].

The methane explosions that have happened since 1983 in Turkey are shown in Table 1 [3].

TABLE 1

Methane explosions occurred in Turkey since 1983

Place	Date	Number of Died
TTK/Armutçuk	7 March 1983	103
TTK/Kozlu	10 April 1983	10
Yeni çeltek/Amasya	14 July 1983	5
TTK/Amasya	31 January 1990	5
Yeni çeltek/Amasya	7 February 1990	63
TTK/Kozlu	3 March 1992	263
Yozgat/Sorgun	26 March 1995	37
Erzurum/Aşkale	8 August 2003	8
Karaman/Ermenek	22 November 2003	10
Çorum/Bayat	9 August 2004	3
Kütahya/Gediz	21 April 2005	18
Balıkesir/Dursunbey	2 June 2006	17
Bursa/Mustafakemalpaşa	10 December 2009	19
Balıkesir/Dursunbey	23 February 2010	13
TTK/Karadon	17 May 2010	30
TOTAL		**636**

Wala and Kim modeled the methane concentration and airflow behavior for seasons in a mine [4]. Edwards et al. researched the application area of CFD to solve the health and safety problems in the mining industry [5].

In the framework of safety in mines, CFD is an accepted approach for enabling the design of ventilation systems that operate in mine galleries. Parra et al. analyzed the flow patterns of different ventilation systems from blowing, suction and mixed configuration using CFD [6]. Kurnia et al. used CFD to simulate the distribution of methane with a blow ventilation system in a mine the tunnel, ensuring the importance of orientating the ventilation jet to the zone of methane emissions instead of ventilating at different locations [7]. The same team of researchers proposed an intermittent ventilation system based on energy savings [8]. Wang et al. performed the numerical analysis of the unsteady ventilation, replicating the dust movement in a diversion tunnel of a real mine in China [9]. The methodology is easily extrapolated to other kinds of mines, like the one conducted by Xie et al. to study the distribution of emissions in uranium mines [10]. Torano et al. modeled the airflow velocity and dust concentration values with a road header taken in 6 different sections from the face (0, 0.5, 3, 6, 12 and 24 m.) and in 6 different points (in 0.5 m. horizontal the plane from the origin, in 1.8 m. the horizontal plane from the origin and 0.5 m. from the roof) using CFD [11]. Wala et al. modeled for face ventilation in room-pillar mining and face ventilation in cut mining that is used during continuous mining [12]

Aminossadi et al. modeled the effect of length of the brattice sail as 2D through a flow-field of a cross-sectional region [13] . Branny investigated the efficiency of methane rarefaction by

the program fluent 6.1. in the longwall-return crossing zone. The air is powerful enough to rarefy effectively [14]. Vlasin et al. presented the computerized simulation deals with the ventilation of a retreating longwall face and highlighted the behavior of methane on the exhaust path [15]. Zhang et al. developed a 3D mine tunnel simulation for the Yin Mu-Si lead and zinc mine [16]. Radui et al. modeled the mechanized face by using fuzzy fraction [17].

Cheng et al. derived the optimum solutions for managing gas hazards and fire risks using CFD in an underground coal seam [18]. Wang et al. investigated methane flow behavior under six different operations and mining conditions [19]. Wang et al. estimated methane emissions from different positions along the face [20]. Lu et al. predicted airflow, methane and coal dust dispersion in a room and pillar mining face [21]. They found the combination of scrubber fan in suction mode and brattice results in methane and dust removal from the mining face. Zhang et al. modeled the respirable dust concentration and air velocity by using CFD in a fully mecha-nis ed mining face [22]. Wachowicz et al. modelled the physicochemical phenomena of the gasification channel using the CFD method for both the Experimental Mine Barbara and the Coal Mine Wieczorek [23]. Skjold et al. improved dust and gas explosions by using the CFD method [24].

CFD modeling studies were conducted at a few underground coal mines and tunnels, but there wasn't a study about coal seams formed under the sea.

Palmer et. al. investigated the differences in properties of Turkish coals. It was found that Black sea coals have a higher fixed-carbon rate than other regions in Turkey [25]. Additionally, it has lower major and trace elements, sulphur, moisture and ash rate [26]. These properties show that Black Sea coals have a higher coal rank and quality than other coals. This factor is an important reason to choose this working area. This study aims to analyze the methane and the airflow behavior in an auxiliary ventilated coal heading in the Kozlu coal mine by using the CFD method. Therefore, this created a numerical model that solves the fluid field (velocity, pressure and concentration). Experimental data is measured with an anemometer and methane gas detector to obtain real values to validate the model.

2. Materials and methods

Computational fluid dynamics uses computers to provide information about how fluids flow in given situations [5,1]. The Navier-Stokes equation assumes steady, incompressible, isothermal, turbulent and non-reactive flow for a three-dimensional model and two species (the methane and the air) [6].

Continuity equation

$$\frac{\partial}{\partial x_i}\left(\underline{\rho u_i}\right) = 0 \tag{1}$$

Momentum equation

$$\frac{\partial}{\partial x_j}\left(\underline{\rho u_i u_j}\right) = -\frac{\partial \underline{p}}{\partial x_i} + \frac{\partial\left(\underline{\tau_{ij}}\right)_{eff}}{\partial x_j} \tag{2}$$

Species conservation

$$\frac{\partial}{\partial x_i}\left(\rho u_i Y_k\right) = \frac{\partial\left(\rho D_{eff}\dfrac{\partial Y_k}{\partial x_j}\right)}{\partial x_j} \tag{3}$$

The term $\left(\tau_{ij}\right)_{eff}$ is the effective stress tensor, which is expressed as:

$$\left(\tau_{ij}\right)_{eff} = \mu\left(\frac{\partial u_i}{\partial x_j} + \frac{\partial u_j}{\partial x_i} - \frac{2}{3}\delta_{ij}\frac{\partial u_k}{\partial x_k}\right) - \rho\overline{u_i' u_j'} \tag{4}$$

The Equations (1) to (3) represent the balance of mass, momentum and species. The $\rho\overline{u_i' u_j'}$ is the Reynolds stress term and it is modeled by utilising the strain tensor, which is based on average velocity, see equation (5).

$$-\rho\overline{u_i' u_j'} = \mu_t\left(\frac{\partial u_i}{\partial x_j} + \frac{\partial u_j}{\partial x_i}\right) - \frac{2}{3}\left(\rho k + \mu_t\frac{\partial u_k}{\partial x_k}\right)\delta_{ij} \tag{5}$$

where μ_t is the eddy turbulent viscosity, then equation (5) is included in equation (4), the Reynolds stress terms can be added to the diffusion term, resulting in an effective viscosity defined as:

$$\mu_{eff} = \mu + \mu_t \tag{6}$$

where the turbulent viscosity is obtained from:

$$\mu_t = \rho \cdot C_\mu \cdot \frac{k^2}{\varepsilon} \tag{7}$$

The standard k-ε turbulence model provides turbulence kinetic energy (k) and its dissipation (ε). The turbulence viscosity and the turbulence conductivity are stated with Eqs. (8)-(9) [27].

$$\frac{\partial}{\partial_t}\left(pk\right) + \frac{\partial}{\partial_{x_i}}\left(pku_i\right) = \frac{\partial}{\partial_{x_i}}\left[\left(\mu + \frac{\mu_t}{\sigma_k}\right)\frac{\partial_k}{\partial x_i}\right] + G_k + G_b + \rho\epsilon - Y_M + S_k \tag{8}$$

$$\frac{\partial}{\partial_t}\left(\rho\epsilon\right) + \frac{\partial}{\partial_{x_i}}\left(\rho\epsilon u_i\right) = \frac{\partial}{\partial_{x_i}}\left[\left(\mu + \frac{\mu_t}{\sigma_\epsilon}\right)\frac{\partial_\epsilon}{\partial_{x_i}}\right] + C_{1\epsilon}\frac{\epsilon}{k}\left(G_k + C_{3\epsilon}G_b\right) - C_{2\epsilon}\rho\frac{\epsilon^2}{k} + S_\epsilon \tag{9}$$

where:

k — Turbulence kinetic energy (m^2/s^2),
ϵ — dissipation of turbulence kinetic energy, (m^2/s^3),
$\rangle$ — Density, (kg/m^3),
μ — Dynamic viscosity, (Pa.s)
μ_t — Turbulence viscosity, (Pa.s)

$\lceil k$, $\lceil \epsilon$ — Turbulence Prandtl constants
$C_{1\epsilon}$, $C_{2\epsilon}$, $C_{3\epsilon}$ — Model constants for k-ε turbulence model
G_b — Turbulence depends on buoyancy
G_k — Turbulence kinetic energy production
Y_M — Turbulence effect of compressibility
$C_{1\epsilon} = 1.44$, $C_{2\epsilon} = 1.92$, $C_\mu = 0.09$, $\sigma_k = 1.0$, $\sigma_\epsilon = 1.3$

2.1. The information on 560 m. Milopera seam in Kozlu-Zonguldak

The Kozlu Hard Coal Establishment is the only facility, which can produce hard coal undersea in Turkey. The facility is located 8 km east of Zonguldak province and has an overall area of 12 km^2 (Fig. 1) [28]. The coal produced in the year 2012 was 704.172 tonnes and the workable coal reserves were 170.260.821 tonnes. Table 2 shows the average coal properties of the mined coal bed.

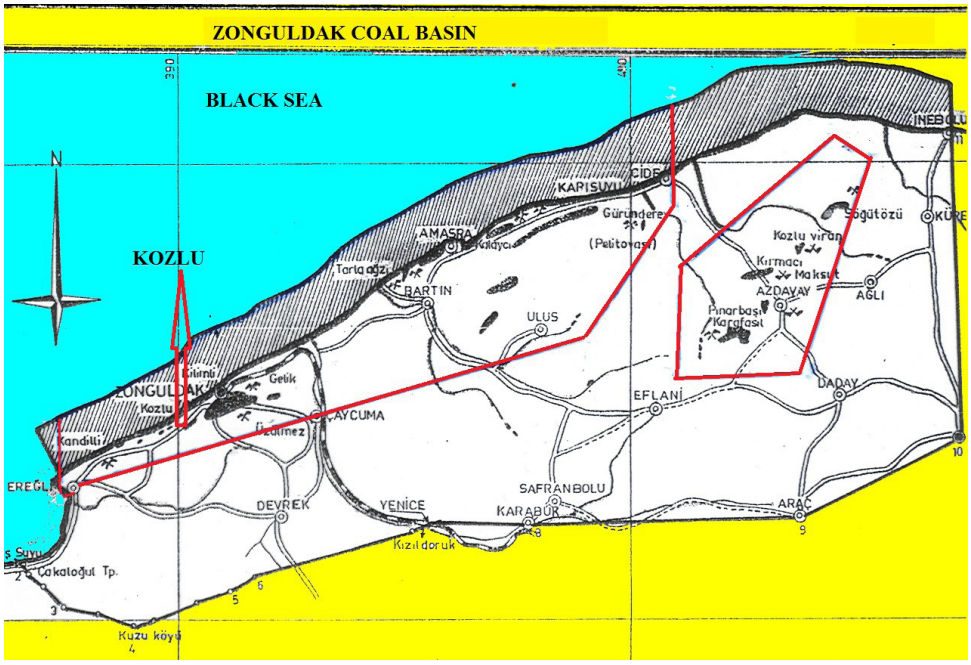

Fig. 1. Zonguldak Coal Basin

TABLE 2

Average coal properties

Ash (%)	Moisture(%)	Volatiles (%)	Fix-carbon(%)	Calorific value (kcal/kg)
12.46	1.74	25.87	59.93	7312

The Kozlu formation is made from approximately 23 coal seams, each with thicknesses between 0.80-10.00 meters and a cumulative thickness of 550-800 meters. It occurred through the Mesozoic-aged, Paleozoic-aged and Carboniferous-aged formations [29]. The produced production is 90% of this formation's seam. Figure 2 shows a stratigraphic column of the Kozlu coal bed.

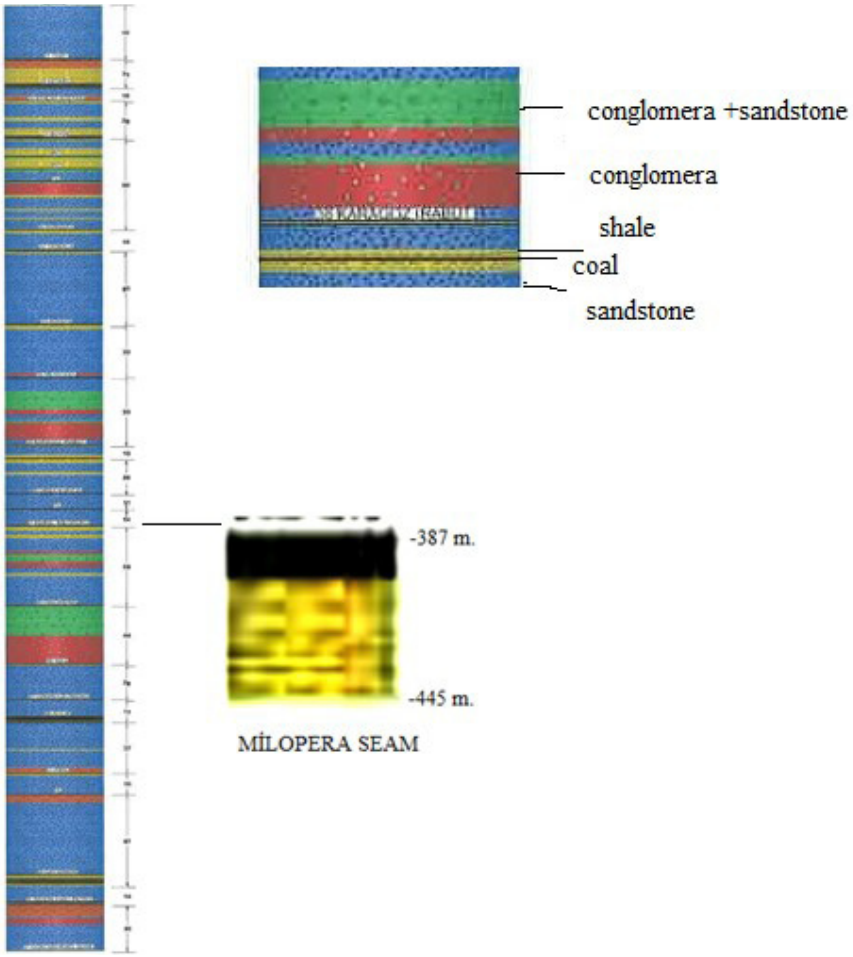

Fig. 2. Stratigraphic column of the mine coal beds

The 560 m Milopera is the deepest and gassiest seam in Kozlu Formation. The thickness of this seam is 3.34 m, and the slope of this seam has a 70° gradient. The reserve amount is 153,000 tonnes, and the production is in progress by pneumatic blasting and tipple. It has an an arched section that is 2.90 m high and 3.50 m wide (9.05 m^2), has an average advance rate per shift of 1.20 m, coal with 12.46% ash content, and a methane concentration in the coal bed of 18.67 m^3/ton. These parameters influence methane emission in this coal bed. Figure 3 shows the coal bed plan.

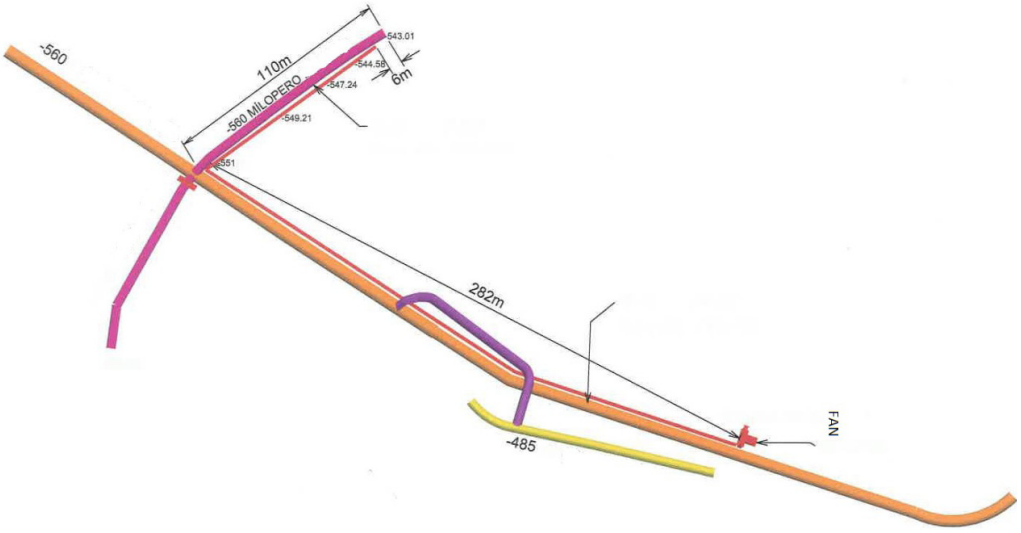

Fig. 3. Plan of 560 m Milopera level

2.2. Experimental set-up

The goal of the experimental analysis is to have usable measurements for numerical model validation. The measurements were taken in Kozlu underground coal mine beneath the Black Sea, Zonguldak, Turkey (Fig. 4). The coal heading is 110 m. long with a quasi semicircular cross-section of 9.05 m^2. The ventilation duct diameter is 0.6 m, and the driven airflow is Q = 2.77 m^3/s.

Fig. 4. Milopera seam in Kozlu (Zonguldak) (TTK)

The height, width and length of coal heading are presented as y, x, z coordinates, respectively. The airflow velocity (m/s) and methane concentration (%) measurements were taken for each cross-section at d1 = 6 m, d2 = 25 m, d3 = 40 m, d4 = 60 m, d5 = 80 m and d6 = 110 m from the coal face. The ventilation duct outlet is placed 6m from the face (Fig. 5).

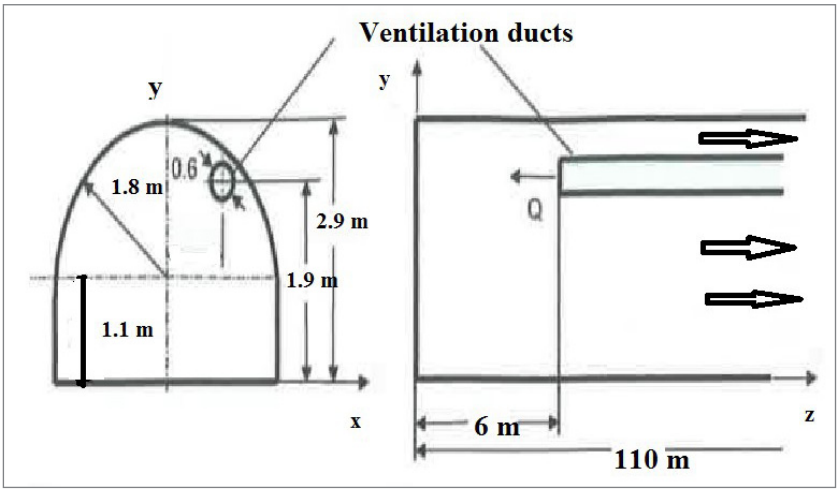

Fig. 5. Plan of the forcing ventilation system

A certified TESTO 435-4 anemometer was used to measure the velocities between 0.20 and 20.00 m/s. Tevel MPS 11D-NG methanometer was used to measure methane values in the mine.

Airflow velocities and methane concentrations were measured in 6 different cross-sections (for each cross-section at 6, 25, 40, 60, and 110 m from the face) and 6 different points between the face of the coal heading and the inlet of the fan (Fig. 6). These values were modeled so they could be compared to the experimental values.

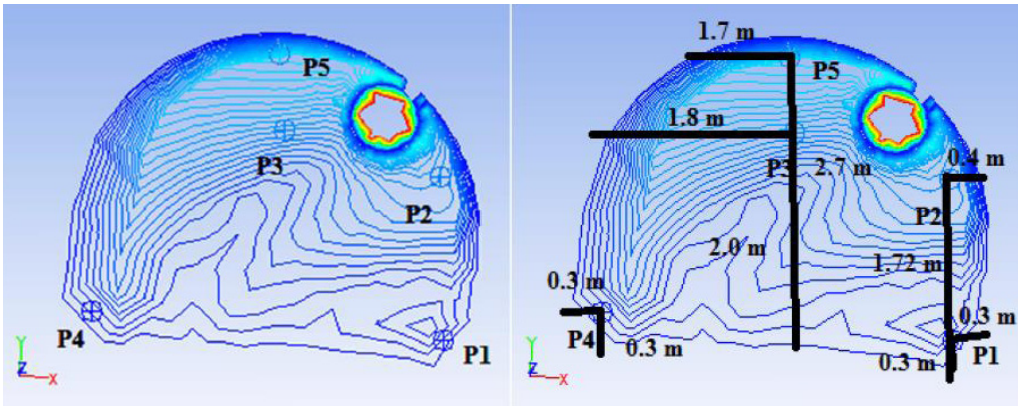

Fig. 6. The contour of velocities of the fixed-point CFD measurements across cross-section

2.3. Numerical model validation

The Ansys-Fluent v.12. commercial software was used to model the two component flow behavior (air-methane) in underground coal headings. The location of the forcing ventilation duct and the same geometrical characteristics for a ductwork and coal heading are taken in to account. The location of the forcing ventilation duct and the same geometrical characteristics for a ductwork and coal heading are taken into account. Three boundary conditions were applied: inlet, outlet and wall. Inlet consists of two parts: one will exist in the ductwork outlet as an airflow velocity, and the other will be in the methane emission from the coal heading face. One inlet is at the forcing duct outlet with an airflow velocity of 9.05 m/s. The second inlet is the methane emission from the coal heading face at 0.098 m^3/s. The opening corresponds to the airflow and methane outlet from the coal heading. The walls are the remaining model surfaces. A tetrahedron type mesh was used in the opening, wall and duct. The mesh interfaces were also increased in the the entry of coal heading.

The model used a tetrahedral mesh comprising 762,844 cells and a mesh quality of 0.8. It is high quality because it is closer to 1.00. Tetrahedral meshes are the best solution in the tunnel geometries [30]. When the CFD model setup was running, it considered the following cases:

1. The mesh number is 762,844 tetrahedral cells, and mesh quality is 0,8. If the mesh quality is near to one, the mesh quality is high in the model. The mesh number should be a medium number (between 700,000 and 800,000).
   Grid sensitive analysis was done for different mesh numbers. It converged to an approximate solution. 760 solutions were converged for 47,768 tetrahedral cells, and 641 solutions were converged for 762,844 tetrahedral cells.
2. The acceleration of gravity (9.81 m/s^2) is active in the model.
3. Parameters of equations are "default" values in the model, such as mass conservation, momentum conservation, energy equation, and species conservation.
4. The k-epsilon turbulence model was selected because many authors, such as Norton et al., Sorensen and Nielsen, Moloney et al., Moloney, Lowrodes, and Torano et al., have determined that the k-epsilon turbulence model offers better results when comparing with experimental data [31].

A segregated solver based on pressure was selected. The SIMPLE pressure velocity coupling and a second-order upwind scheme were used to carry out the simulation. Because y+ is higher than 30 near the walls, the logarithmic boundary layer is imposed on the cells in contact with walls to predict the velocity. y+ is a non-dimension distance dependent on the mesh, and it states the cell region. There are three regions in a limit layer: laminar sub-layer ($y^+ < 5$), buffer region ($5 < y^+ < 30$) and turbulent region ($y^+ > 30$) [32]. The computational domain is characteris ed by a flow (air) at 27° C and the humidity and the heat have not been taken into consideration. The barometric pressure is 105,85 kPa. The simulations were carried out with a k-epsilon model. Neither the humidity nor the heat transfer effects have been taken into account. The accuracy of the model can be proved at the "flux reports" panel in the programm after a certain number of iterated convergences. According to flux reports, if the difference between inlet and outlet mass flow rate near zero, then the model is correct [32]. The "net results" between inlet and outlet mass flow rate was found to be 0.000983797 (kg/sn) for this model. This value shows the accuracy of the model. The average experimental and CFD values are shown in 5 points of 5 cross-sections in Table 3.

TABLE 3

Average experimental and CFD values in 5 points of 5 cross-sections

Cross-section	Results	Average air velocity (m/s)					Average methane concentration (%)				
		Points					Points				
		P1	P2	P3	P4	P5	P1	P2	P3	P4	P5
6 m	CFD	0.955	1.20	1.1	1.204	2.167	0.317	0.435	0.483	0.314	0.573
	Exp.	1.1	0.80	0.48	0.11	0.14	1.00	1.00	1.00	1.00	1.1
25 m	CFD	0.29	0.049	0.327	0.626	0.338	0.385	0.427	0.453	0.384	0.473
	Exp.	0.13	0.26	0.332	0.26	0.38	0.75	0.7	0.7	0.7	0.75
40 m	CFD	0.385	0.049	0.241	0.626	0.241	0.372	0.425	0.423	0.374	0.473
	Exp.	0.446	0.48	0.28	0.28	0.44	0.7	0.7	0.7	0.7	0.7
60 m	CFD	0.385	0.049	0.337	0.722	0.241	0.413	0.426	0.43	0.423	0.423
	Exp.	0.37	0.46	0.311	0.34	0.31	0.7	0.7	0.7	0.7	0.7
110 m	CFD	0.193	0.337	0.626	0.434	0.53	0.422	0.428	0.43	0.413	0.423
	Exp.	0.46	0.42	0.445	0.48	0.33	0.7	0.7	0.7	0.7	0.7

3. Results

3.1. Comparison of the experimental and CFD modeling results of airflow and methane measurements

The methane concentration values and airflow velocity measurements were taken for each cross-section at 6, 25, 40, 60, 110 m. from the face. The experimental and CFD modeling are shown below (Figs 7-11).

According to the three-dimensional model, the methane concentration and airflow velocity values were taken for each cross-section at 6, 25, 40, 60, 110 m from the face. The methane gas accumulates in the roof of the coal heading, and it is the highest value at a 6 m distance from the face (Fig. 7). It decreases again from the roof to the floor at 6, 25, 40, 60, 110 m from the face

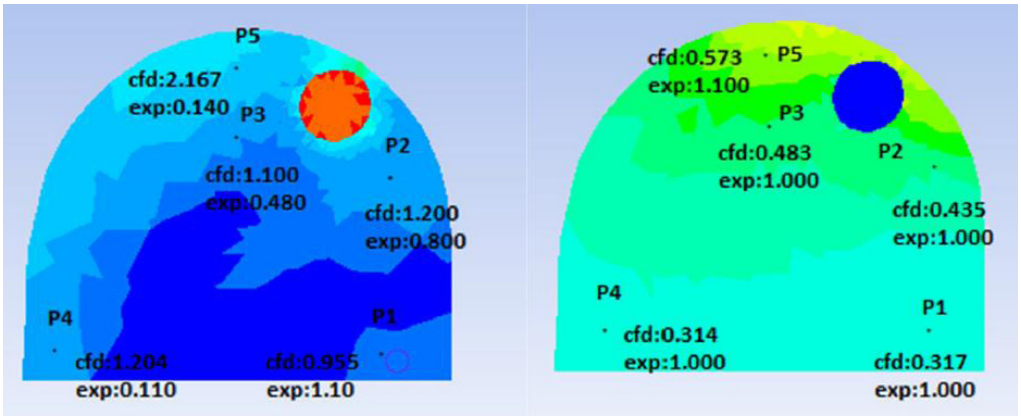

Fig. 7. Contour of the airflow velocity and methane concentration for 5 points in 6 m distance from the face

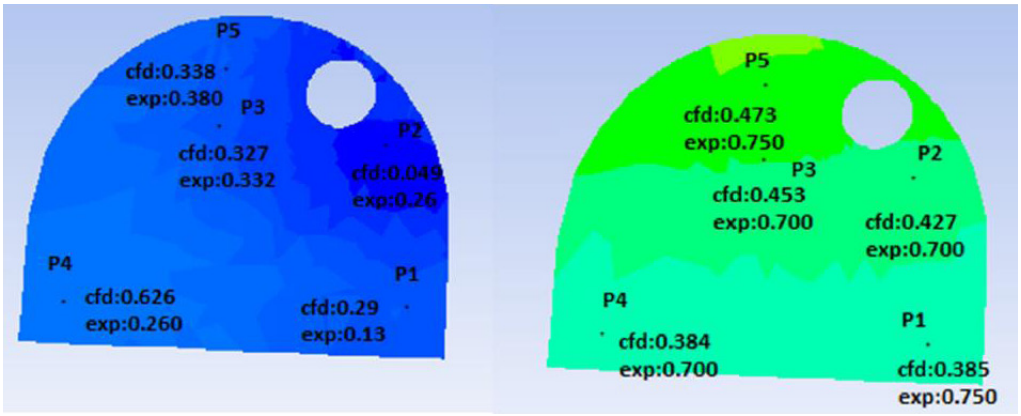

Fig. 8. Contour of the airflow velocity and methane concentration for 5 points in 25 m distance from the face

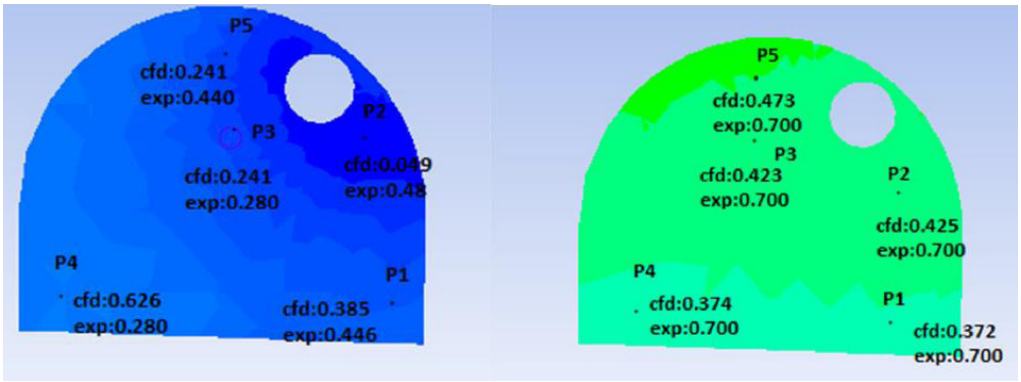

Fig. 9. Contour of the airflow velocity and methane concentration for 5 points in 40 m distance from the face

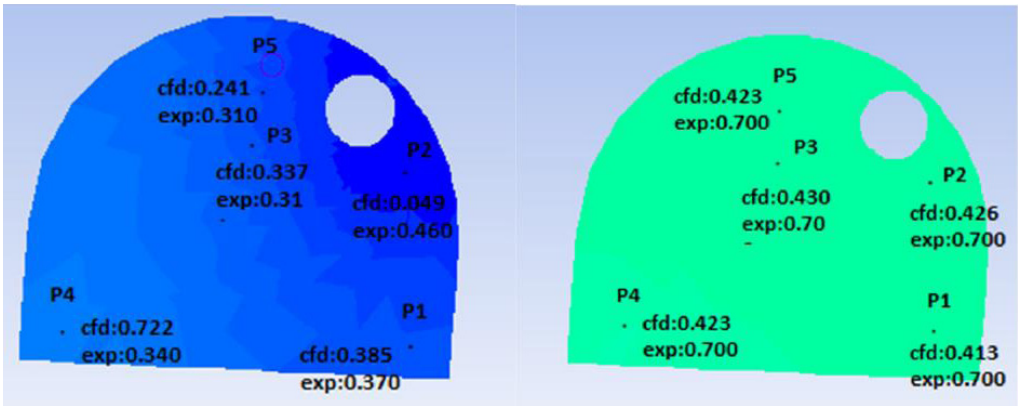

Fig. 10. Contour of the airflow velocity and methane concentration for 5 points in 60 m distance from the face

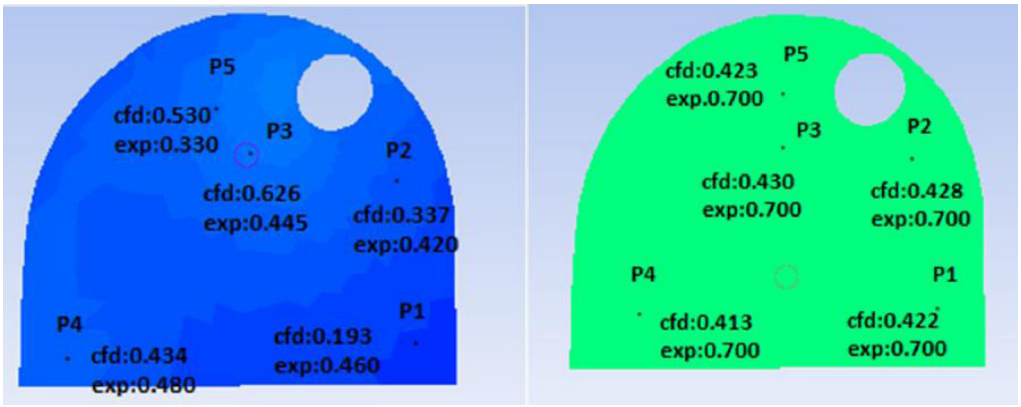

Fig. 11. Contour of the airflow velocity and methane concentration for 5 points in 110 m distance from the face

(Figs 8-11). The methane reaches a certain value for both experimental (0.43) and CFD (0.70) from a distance of 60m to 110 m from the face (Figs 10-11). Namely, the methane equally diffuses at a certain distance in the coal heading. The airflow behavior is lower near the face and higher in the duct outlet (Fig. 8). The duct is located at a distance of 6m from the face, where initially it comes across the airflow and methane gas. Experimental and modelling airflow values deviated because of the intense turbulence effect. For example, the values associated with points 2 and 4 were far apart from one another at a distance of 25 m from the face. Whereas, for points 1, 3, and 5 the values were close to each other. There is an intense turbulence flow at point 22 under the duct. Additionally, when the literature is examined, significant differences are noticed between the measured and modeled air velocity values, especially near the face (at a 6 m distance). Pollutants are denser than air, such as carbon dioxide and nitrous oxide, on the bottom-left corner (at point 4) for 6 m and 25 m distance from the face. Points 1, 2, and 3 deviate from the effect of high turbulence and point 4 deviates from the effect of heavy gases from the air at a 6m distance from the face. Then, it shows isometric dispersion. Mainly, it decreases from the left-floor bottom to the center and increases from the center to the right-floor bottom (Figs 9-11).

3.2. Assessment of test results with statistical analysis

A hypothesis test was performed in order to determine whether there was any difference between modeling and experimental values of air velocity and the methane measurements in every point (P1, P2, P3, P4, P5) separately. A One-Way ANOVA test was applied to compare the significant difference between each modeling and experimental means for every point. The Minitab-17 statistics package programm was used for comparing mean differences in more than two groups. In the hypothesis test for velocity:

H_0: There is no significant difference between each modeling and experimental air velocity means at every point.

H_1: There is a significant difference between each modeling and experimental air velocity means at every point.

The significant F values of every point (P1, P2, P3, P4, P5) tell us that at least the air velocity values group effect differs from zero, i.e. the means are not all equal. Results from the ANOVA table, which accepted the H1 hypothesis, was performed to investigate whether there was any difference between CFD and experimental air velocity means from the highest F-test values and are presented with the P values < α (coefficient level) = 0.05 in Table 4.

TABLE 4

Analysis of variance for air velocity values in every point between CFD and experimental groups

Point	Source	df	SS	MS	F	Prob < F
1	Regression	1	0.28522	0.28522	12.30	0.039
	Error	3	0.06955	0.02318		
	Total	4	0.35477			
2	Regression	1	0.77621	0.77621	10.38	0.049
	Error	3	0.2243	0.07477		
	Total	4	1.0005			
3	Regression	1	0.43012	0.43012	19.58	0.021
	Error	3	0.06590	0.02197		
	Total	4	0.49602			
4	Regression	1	0.26345	0.26345	11.25	0.044
	Error	3	0.07025	0.02342		
	Total	4	0.33370			
5	Regression	1	2.2574	2.2574	14.23	0.033
	Error	3	0.4760	0.1587		
	Total	4	2.7333			

In the hypothesis test for methane:

H_0: There is no significant difference between each modeling and experimental methane means at every point.

H_1: There is a significant difference between each modeling and experimental methane means at every point.

The significant F values of every point (P1, P2, P3, P4, P5) tell us that at least the methane values group effect differs from zero, i.e. the means are not all equal. Results from the ANOVA table, which accepted the H1 hypothesis and was performed to investigate whether there was any difference between CFD and experimental air velocity means from the highest F-test values, are presented with the P values < α (coefficient level) = 0.05 in Table 5.

Table 6 shows the correlation coefficient and the determination coefficient of the average methane concentration value (%) and the average airflow velocity value (m/s). When the determination coefficients (R2) of every point are closer to 100%, the relationship between variables is stronger. Because the correlation coefficients (r) of every point is closer to 1.00, there is a positive and significant correlation between experimental and modeling methane values and air velocity values [33].

TABLE 5

Analysis of variance for methane values in every point between CFD and experimental groups

Point	Source	df	SS	MS	F	Prob < F
1	Regression	1	0.005466	0.005466	11.48	0.043
	Error	3	0.001428	0.000476		
	Total	4	0.006895			
2	Regression	1	0.000058	0.000058	34.68	0.010
	Error	3	0.000005	0.000002		
	Total	4	0.000063			
3	Regression	1	0.001921	0.001921	11.21	0.044
	Error	3	0.000514	0.000171		
	Total	4	0.002435			
4	Regression	1	0.005712	0.005712	10.57	0.047
	Error	3	0.001621	0.000540		
	Total	4	0.007333			
5	Regression	1	0.013115	0.013115	20.87	0.020
	Error	3	0.001885	0.000628		
	Total	4	0.015000			

TABLE 6

The correlation and determination coefficients of average methane and airflow velocity

Point	Average methane concentration value		Average airflow velocity value	
	Correlation coefficient (r)	Determination coefficient (R^2)	Correlation coefficient (r)	Determination coefficient (R^2)
1	–0.89	79.3	0.897	80.4
2	0.958	92.0	0.881	77.6
3	0.888	78.9	0.931	86.7
4	–0.883	77.9	–0.889	78.9
5	0.935	87.4	–0.909	82.6

4. Discussion

In this study, the methane and the airflow behavior were modeled by the CFD method in a coal mine. Mean-good mesh, gravitation acceleration, and default values were implemented for accurate modeling. The methane accumulates in the roof of the coal heading and it decreases from the roof to the floor at 6, 25, 40, 60 and 110 m from the face. It was found that the methane concentration values were high in the roof of the cross-section which didn't have the duct. The methane value reaches a certain level for both experimental (0.43) and CFD (0.70) from 60 m to 110 m from the face. An additional fan can be used at this point due to the decrease in the amount of methane. The airflow behavior is lower near the face and higher in the duct outlet. It shows isometric dispersion. According to the analysis of variance, there is a significant correlation

between the experimental and modeling values for methane and air velocity at a 95% confidence level. The determination coefficient (R^2) of average airflow velocity values were between 77.6-86.7(%), and the determination coefficient (R^2) of average methane concentrations values were 77.9-92.0 (%). There is a very high correlation between experimental and modelling values. Thus, the CFD method is developed using various parameters to prevent coal mine accidents even if methane values fluctuate in a day.

Acknowledgement

This study has been supported by the Scientific and Technological Research Council of Turkey (TUBITAK) between 2012-2013. The authors wish to acknowledge the help from TUBITAK, all of the workers in the Turkish Hard coal enterprises (TTK), Pejman KAZEMPOOR, Erdinç GÜNAY, Özlem SEKMEN, and Olgun ESEN.

References

[1] J. Toraño, S.Torno, M. Menendez, M. Gent, J. Velasco. Int. J. of Coal Geology **80** (1), 35-43 (2009).

[2] J.K. Richmond, G.C. Price, M.J. Sapko, E.M. Kawenski, *Historical summary of coal mine explosions in the United States 1959-1981*. In: Bureau of Mines Information Circular (IC-8909), (1983).

[3] The Chamber of Mining Engineers of Turkey (TMMOB), The Occupational Accidents Report in Mining, Turkey (2010).

[4] A.M. Wala, B.J. Kim, *Simulation of unsteady-state of airflow and methane concentration processes in mine ventilation systems caused by disturbances in main fan operation*. In: Mopusset-Jones (Eds.), the Second US Mine Ventilation Symposium, (1985).

[5] J.S. Edwards, T.X. Ren, R. Jozefowicz, *Using CFD to solve mine safety and health problems*. In: APCOM XXV Conference, Brisbane, (1995).

[6] M.T. Parra, J.M. Villafruela, F. Castro, C. Méndez, Building and Env. **41** (2), 87-93 (2006).

[7] J.C. Kurnia, A.P. Sasmito, A.S. Mujumdar, Appl. Mathematical Modelling **38**, 3467-3484 (2014).

[8] J.C. Kurnia, A.P. Sasmito, A.S. Mujumdar, Tunnelling and Underground Space Technology **42**, 206-215 (2014).

[9] X. Wang, X. Liu, Y. Sun, J. An, J. Zhang, H. Chen, J. of Hazard Materials **165,** 933-943 (2009).

[10] D. Xie, H. Wang, K.J. Kearfott, Z. Liu, S. Mo, J. of Env. Radioactivity **129**, 57-62 (2014).

[11] J. Toraño, S. Torno, M. Menendez, M. Gent, Tunnelling Underground Space Technology **26**, 201-210 (2011) .

[12] A.M. Wala, J.C. Yingling, J. Zhang, *Evaluation of the face ventilation systems for extended cuts with remotely operated mining machines using three-dimensional numerical simulations*. In: Metall. and Exploration Annual Meeting Society for Mining, (1998).

[13] S.M. Aminossadati, K. Hooman, *Numerical simulation of ventilation air flow in underground mine workings*. In: 12th U.S./North American Mine Ventilation Symposium, 253-259 (2008).

[14] M. Branny, *Computer simulation of flow of air and methane mixture in the longwall-return crossing zone*. Petroleum Journals Online, 1-10 (2007).

[15] N.I. Vlasin, C. Lupu, M. Şuvar, V.M. Pasculescu, S. Arad, *Computerised modelling of methane releases exhaust from a retreating logwall face*. In: 4th European Conference on Recent Advances in Civil and Mining Engineering (ECCIE'13), 274-277 (2013).

[16] Z.H. Zhang, E.K. Hov, N.D. Deng, J.H. Guo, *Study on 3D mine tunnel modelling*. In: the International Conference on Environment, Ecosystem and Development (EED'07), 35-40 (2007).

[17] S.M. Radui, G. Dolea, R. Cretan, *Modeling and simulation of coal winning process on the mechanized face*. In: 4th European Conference on Recent Advances in Civil and Mining Engineering (ECCIE'13), 30-35 (2013).

[18] J. Cheng, S. Li, F. Zhang, C. Zhao, S. Yang, A. Ghosh, J. of Loss Prevention in the Process Industries **40**, 285-297 (2016).

[19] Z. Wang, T. Ren, Y. Cheng, J. of Naturel Gas Science and Engineering **43**, 254-267 (2017b).

[20] Z. Wang, T. Ren, Y. Cheng, J. of Naturel Gas Science and Engineering **43**, 242-253 (2017a).

[21] Y. Lu, S. Akhtar, A.P. Sasmito, J.C. Kurnia, Int. J. of Mining Science and Technology **27**, 657-662 (2017).

[22] Q. Zhang, G. Zhou, X. Qian, M. Yuan, Y. Sun, D. Wang, J. of Cleaner Production **184**, 239-250 (2018).

[23] J. Wachowicz, J.M. Laczny, S. Iwaszenko, T. Janoszek, M. Cempa-Balewicz, Arch. Min. Sci. **60**, 663-676 (2015).

[24] T. Skjold, D. Castellanos, K.L. Olsen, R.K. Eckhoff, J. of Loss Prevention in the Process Industries **30**, 164-176 (2014).

[25] C.A. Palmer, E. Tuncalı, K.O. Dennen, T.C. Coburn, R.B. Finkelman, Int. J. Coal Geology **60**, 85-115 (2004).

[26] S. Toprak, Int. J. of Coal Geology **78,** 263-275 (2009).

[27] A.E. Karkınlı, T. Kurban, A. Kesikoglu, E. Beşdok, *CFD based risk simulations and management on CBS*. In: Congress of Geographic Information Systems, Antalya, Turkey (2011).

[28] http://www.theatc.org/events/cleanenergy/pdf/TuesdayMorningBallroom2&3/Bicer, accessed: 09.05.2012.

[29] Turkish Hard Coal Enterprises (TTK), Turkish Hard Coal Enterprise general management activities between 2003 and 2009, (2009).

[30] I. Diego, S. Torno, J. Torano, M. Menendez, M. Gant, Tunnelling Underground Space Technology **26**, 189-200 (2011).

[31] S. Torno, J. Torano, M. Ulecia, C. Allende, Tunnelling Underground Space Technology **34**, 73-81 (2013).

[32] Z. Altaç, *Modeling Samples with Gambit and Fluent*. Depart. of the Mech. Eng. of Eskisehir Osmangazi Univ., Turkey (2005).

[33] A. Konuk, S. Önder, *Statistics for Mining Engineers*. Depart. of the Mining Eng. of Eskisehir Osmangazi Univ., Turkey (1999).